Supporting Information for:

Structure and Dynamics of Cinnamycin-Lipid Complexes: Mechanisms of Selectivity for Phosphatidylethanolamine Lipids

Mikkel Vestergaard#, Nils Anton Berglund#, Pin-Chia Hsu#, Chen Song‡1,2, Heidi Koldsø‡,1, Birgit Schiøtt#, and Mark S.P. Sansom‡**

‡Department of Biochemistry, University of Oxford, South Parks Road, OX1 3QU Oxford, United Kingdom

#Center for Insoluble Protein Structures (inSPIN), Interdisciplinary Nanoscience Center (iNANO), Department of Chemistry, Aarhus University, Langelandsgade 140, DK-8000 Aarhus C, Denmark

*To whom correspondence should be addressed:

Birgit Schiøtt: birgit@chem.au.dk; Phone +45 29826882

Mark Sansom: mark.sansom@bioch.ox.ac.uk; Phone: +44 (0)1865 613212

[1]current address:

C.S. – 1 Center for Quantitative Biology, Academy for Advanced Interdisciplinary Studies, Peking University, Beijing 100871, People's Republic of China

C.S. – 2 Peking-Tsinghua Center for Life Sciences, Academy for Advanced Interdisciplinary Studies, Peking University, Beijing 100871, People's Republic of China

H.K - Schrödinger, 120 W. 45th St., 17th Fl., New York, NY 10036, USA

Methods

All simulations were conducted with GROMACS 4.6.5[1,2] at a temperature of 310 K and a pressure of 1 bar. The CHARMM36 force field[3,4] was employed for all atomistic simulations and residues not already present in the force field were constructed by analogy to other molecules in the CHARMM36 protein force field[3] or the CHARMM general force field.[5] The parameters used for the *erytho*-3-hydroxy-L-aspartic acid (HyAsp) was a combination of the parameters for aspartic acid and threonine while parameters related to the new *meso*-lanthionine (Lan) and (2*S*,3*S*,6*R*)-3-methyllanthionine (MeLan) side chain bonds were made from analogy to primary methionine. Parameters from CHARMM general force field were used for the bonding between lysine and the deoxylated serine in (2*S*,8*S*)-lysinoalanine (LysAla) as well as other missing bonded terms. Charges for the lipid head group were predicted with paramchem 0.9.7.1,[6,7] while bonded terms were taken from POPE and POPC. All the added topologies and parameters are listed in Table S1-3 and Figure S1 in GROMACS format.

Table S1. Bond parameters added to the CHARMM36 force field.

Bonds:	Function type	B_0 (nm)	K_b (kJ/mol/nm^2)	From:
S-CT1	1	0.1818	165686.4	S-CT2
NH3L-CTL5	1	0.151	179912	NTL-CTL5

Table S2. Angle parameters added to the CHARMM36 force field.

Angles:	***Function type***	ϑ_0 ***(deg)***	k_ϑ **(kJ/mol/rad^2)**	r_{13} ***(nm)***	k_{UB} **(kJ/mol/nm^2)**	***From:***
CT2-S-CT2	5	95	284.512	0	0	CT3-S-CT2
CT1-S-CT2	5	95	284.512	0	0	CT3-S-CT2
HA1-CT1-CC	5	109.5	276.144	0.2163	25104	HA1-CT1-C
NH3-CT2-CT1	5	110	566.5136	0	0	NH3-CT2-CT2
S-CT1-CT1	5	112.5	485.344	0	0	S-CT2-CT1
S-CT1-CT3	5	114.5	485.344	0	0	S-CT2-CT3
S-CT1-HA1	5	111.3	385.7648	0	0	S-CT2-HA2
CC-CT1-OH1	5	109	376.56	0	0	CG2O3-CG311-OG301
CT2-NH3-CT2	5	115.2	334.72	0	0	CG324-NG3P2-CG324
NH3L-CTL5-HL	5	109.5	334.72	0.213	22593.6	NTL-CTL5-HL
CTL5-NH3L-CTL2	5	109.5	502.08	0.2466	21756.8	CTL5-NTL-CTL2
CTL5-NH3L-CTL5	5	109.5	502.08	0.2466	21756.8	CTL5-NTL-CTL5
HCL-NH3L-CTL5	5	109.5	276.144	0.2056	3347.2	HCL-NH3L-CTL2

Table S3. Dihedral parameters added to the CHARMM36 force field.

Dihedrals:	***Function type***	***φ_0 (deg)***	***K_φ (kJ/mol)***	***Multipli-city***	***From:***
CT2-S-CT2-CT1	9	180	1.00416	1	CT3-S-CT2-CT2
CT2-S-CT2-CT1	9	0	1.54808	3	CT3-S-CT2-CT2
CT2-S-CT1-CT1	9	180	1.00416	1	CT3-S-CT2-CT2
CT2-S-CT1-CT1	9	0	1.54808	3	CT3-S-CT2-CT2
CT2-S-CT1-CT3	9	180	1.00416	1	CT3-S-CT2-CT2
CT2-S-CT1-CT3	9	0	1.54808	3	CT3-S-CT2-CT2
CT1-S-CT2-CT1	9	180	1.00416	1	CT3-S-CT2-CT2
CT1-S-CT2-CT1	9	0	1.54808	3	CT3-S-CT2-CT2
HA2-CT2-S-CT1	9	0	1.17152	3	HA2-CT2-S-CT3
HA1-CT1-S-CT2	9	0	1.17152	3	HA2-CT2-S-CT3
HA2-CT2-S-CT2	9	0	1.17152	3	HA2-CT2-S-CT3
S-CT1-CT3-HA3	9	0	0.04184	3	S-CT2-CT2-HA2
HB1-CT1-CT2-NH3	9	0	0.8368	3	HB1-CT1-CT2-CT3
HB1-CT1-CT1-S	9	0	0.8368	3	HB1-CT1-CT2-S
HA1-CT1-CC-OC	9	180	0.2092	6	HA2-CT2-CC-OC
C-CT1-CT1-S	9	180	1.00416	1	C-CT1-CT2-S
C-CT1-CT1-S	9	180	3.138	2	C-CT1-CT2-S
C-CT1-CT1-S	9	180	5.6484	3	C-CT1-CT2-S
NH1-CT1-CT1-S	9	0	1.42256	1	NH1-CT1-CT2-S
NH1-CT1-CT1-S	9	180	2.092	2	NH1-CT1-CT2-S
NH1-CT1-CT1-S	9	0	5.98312	3	NH1-CT1-CT2-S

NH1-CT1-CT2-NH3	9	0	0.81588	3	NG2S1-CG311-CG324-NG3P2
NH3-CT2-CT1-C	9	0	0.8368	3	NG3P3-CG314-CG321-CG2O1
X-CTL5-NH3L-X	9	0	0.96232	3	X-CTL5-NTL-X
X-HCL-NH3L-X	9	0	0.96232	3	X-CTL5-NTL-X
C-CT1-CT1-CC	9	180	6.73624	1	C-CT1-CT2A-CC
C-CT1-CT1-CC	9	180	5.39736	2	C-CT1-CT2A-CC
C-CT1-CT1-CC	9	180	2.46856	3	C-CT1-CT1-CC
CC-CT1-CT1-NH1	9	180	2.84512	1	CC-CT2A-CT1-NH1
CC-CT1-CT1-NH1	9	180	0.4184	2	CC-CT2A-CT1-NH1
CC-CT1-CT1-NH1	9	0	1.58992	3	CC-CT2A-CT1-NH1
CT1-CT1-CC-OC	9	0	3.51456	1	CT1-CT2A-CC-OC
CT1-CT1-CC-OC	9	180	4.10032	2	CT1-CT2A-CC-OC
CT1-CT1-CC-OC	9	0	6.10864	3	CT1-CT2A-CC-OC

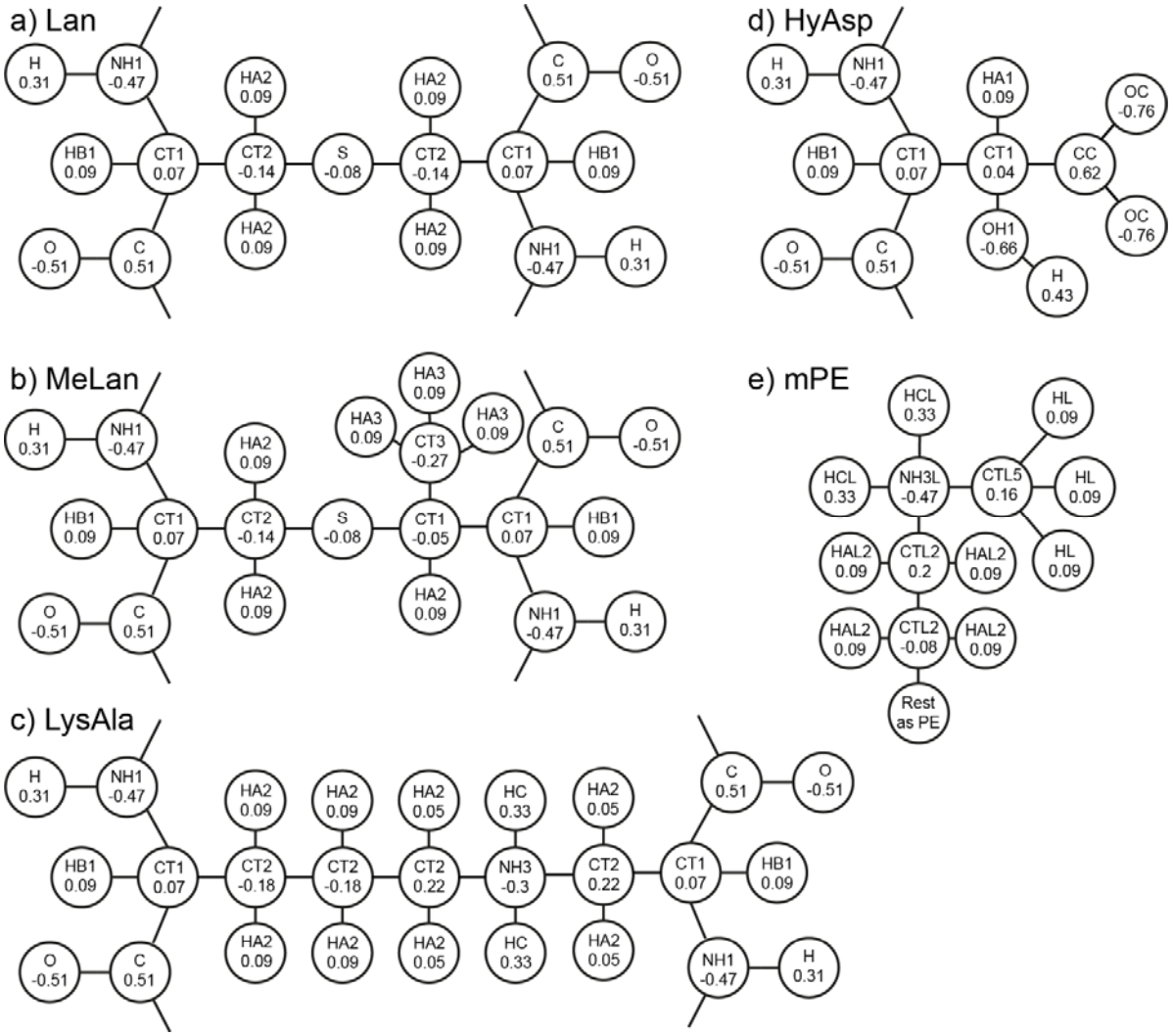

Figure S1. Atom types and charges of the residues and mPE lipid added to the CHARMM36 force field.

Water molecules were described by the TIPS3P water model developed for CHARMM.[8,9] During equilibration the Berendsen thermostat and barostat[10] were used with a τ_p and τ_t of 1 ps and a compressibility of 4.5×10^{-5} bar^{-1}. The production runs were conducted with a Nosé-Hoover thermostat[11] and a Parinello-Raman barostat[12] with the time constants τ_t and τ_p of 1 ps and with a compressibility of 4.5×10^{-5} bar^{-1}. The pressure in solvent simulations was controlled isotropically while a semiisotropic

pressure coupling was employed in bilayer simulations with the dimension perpendicular to the bilayer controlled independently from the other two. The bonds in the water molecules were constrained with SETTLE,[13] while other bond lengths involving hydrogens were constrained with a LINCS algorithm[14] hereby allowing for a time step of 2 fs. Periodic boundary conditions were employed and the neighbor list had a cutoff of 1.4 nm and was updated every ten steps. Electrostatic interactions were calculated by use of particle mesh Ewald (PME)[15] with a real space cutoff of 1.4 nm and a reciprocal spacing of 0.15 nm^{-1}. The Lennard-Jones potential was turned off using a shift-function from 1.0 to 1.2 nm. Snapshots were stored every 10 ps and used for the analyses.

Solvent simulations

Simulations of cinnamycin in different solvents with 1,2-dilauroyl-*sn*-glycero-3-phosphocholine (DLPE) bound were initially constructed by starting from the published NMR structure (PDB-code 2DDE, model 1)[16], converting the lysophosphatidylethanolamine therein into DLPE and solvating the complex in a 5 nm x 5 nm x 5nm solvent box. In the initial simulations, the systems were equilibrated for 1 ns followed by a 300-ns production run (simulations named D_{NMR}, W_{NMR}, and E_{NMR}). However, as the complex was found to be unstable another approach was needed. Therefore, another set of simulations were conducted where the systems were subjected to 1 ns equilibration followed by four consecutive 10 ns simulations with restraints between atoms of the lipid and the peptide derived from NOEs (see Figure 2).[17] Force constants of 1000, 100, 10, and 1 kJ/mol/nm^2 were used for the equilibration and the four consecutive simulations, respectively. The different solvents were selected for the following reasons: DMSO was chosen to match the solvent in which the NMR structure was determined;[16] water is the most common solvent applied; and, since DMSO had not been parameterized in the MARTINI coarse-grained (CG) force field, ethanol (that have similar properties to DMSO such as lower dielectric constant

compared to water) was used to develop the CG parameters used in self-assembling a bilayer around cinnamycin.

Bilayer simulations

To access how cinnamycin is embedded in a lipid bilayer, self-assemble simulations with the MARTINI 2.2 CG force field[18,19] were conducted as described below. Two of the formed POPC bilayer and three of the 80:20 POPE:POPG bilayer with cinnamycin-POPE complex embedded were converted to an atomistic description by use of the Backward Tool.[20] The conformation of cinnamycin and the head group of the bound lipid was taken from D_{flip} and exchanged for the equivalent CG structures to initiate the simulations from a model fitting the observed NOEs[17] the best way possible. The 80:20 POPE:POPG membranes were used to model a bacteria membrane as it is approximately the lipid composition in *E. coli* cells.[21]

All systems, except half of each of the simulations named *PE_HyAsp*, *mPE_HyAsp*, *PC_HyAsp*, and *PS_HyAsp*, and the simulations named *PE_HyAsp_PEPG*, were equilibrated for 1 ns followed by 4 x 10 ns with the NMR derived restraints previously described. The systems not equilibrated with this protocol were instead equilibrated for 1 ns with the protein backbone position restrained. These variations were made to test if the equilibration protocol affected the results. However, no significant effect was observed from the difference in equilibration, because the complex was already in a stable conformation. They will therefore here be presented together independent of the used equilibration protocol. The equilibration was followed by 500 ns of simulations without restraints. Besides cinnamycin and the bound lipid the systems contained 99 lipids (POPC or 79:20 POPE:POPG), 6000 water molecules, and ions to give a electroneutral system (no ions with PS bound, 1 chloride ion and 20 sodium ions with PE bound in the POPE:POPG bilayers and 1 chloride ion in all other setups).

As the NMR restraints indicate that the HyAsp15 χ1 side chain angle should be in the gauche(+) conformation, simulations were conducted with the HyAsp15/Asp15 χ1 angle restrained to the interval 0-100° with a force constant of 100 kJ/mol/rad^2 (denoted with *HyAsp*$^+$ or *Asp*$^+$ in Table 2). Likewise, simulations with restraints on the ψ-angle of Ala(N)6 (retained between -130 and 50°) or the ϕ-angle of Gly8 (between 50 and 230°) were performed with a force constant of 100 kJ/mol/rad^2 (denoted with *Ala(N)6* and *Gly8* in Table 2, respectively). These simulations were carried out to evaluate the effect of fixing the orientation the Phe7(H_N) or Phe7(O), respectively, which may be important for lipid binding as we find that this residue takes part in the hydrogen binding network formed upon complex formation.

Coarse-Grained Self-assembling

For the CG simulations the MARTINI 2.2 force field was employed.[18,19] The β-hydroxyaspartic acid was modelled in the same way as an aspartic acid except that the side chain bead was modelled by a Q_{ad} instead of a Q_a bead as the hydroxyl group acts as both a hydrogen bond donor and acceptor. Bonded terms for new residues were taken from equivalent standard residues, however some changes were needed for residues with side chain crosslinking: The cysteine side chain bead taking part in the Lan and MeLan residues was made to also include the C_β atom of the connected residue, the lysine SC2 side chain bead was made to include the C_β of the connected alanine residue in LysAla, and no independent side chain bead was therefore modelled for the connected residue. These changes made it necessary to increase the bond length in respect to these residues as described in Table S4. Furthermore, to account for the bonds between the side chains, bonded parameters were added as specified in Table S4. These parameters were derived to fit the equivalent angle and distance distributions of atomistic simulations of cinnamycin in ethanol and water. The angle and length distributions were derived from the last 500 ns

of three 1000 ns atomistic simulations and one 1000 ns CG simulation in both water and ethanol simulations. Secondary structure was determined by DSSP[22] of the NMR model.

Table S4. CG parameters added/changed for unusual amino acids.

Bond lengths[a]	***Distance (nm)***	***Force constant (kJ/mol/nm)***
AXX(S)(BB)- AXX(S)(SC1)	0.33	7500
Lys(SC1)-Lys(SC2)	0.34	5000
Lys(SC2)-Ala(N)(BB)	0.33	5000
Angles[a]	***Angle (degrees)***	***Force constant (kJ/mol/rad)***
AXX(S)(SC1)- AXX(S)(BB)- AXX(S)$_{-1}$(BB)	100	25
Lys(SC2)-Ala(N)(BB)- Ala(N)$_{-1}$(BB)	100	25
Lys(SC1)-Lys(SC2)- Ala(N)(BB)	180	25
AXX(S)(BB)- AXX(S)(SC)- AXX(S)(BB)	140	25

(a) X$_{-1}$(BB) specifies the residue ahead of the uncommon residue in the sequence. AXX(S) refers to both Ala(S) and Abu(S), as these are modelled in the same way in CG.

All CG simulations were conducted with a 25 fs time step. The neighbor list was cut off at 1.4 nm and updated every ten steps. The van der Waals interactions were switched off from 0.9 to 1.2 nm while the Coulomb interactions were turned off from 0 to 1.2 nm, both by use of a shift function. All setups were minimized and equilibrated for 100 ns (with the Berendsen thermostat and barostat as described for the atomistic simulations) followed by production runs conducted with the v-rescale thermostat[23] with a τ_t of 1 ps and the Parinello-Raman barostat[12] with a τ_p of 12 ps and a compressibility of 3×10^{-4} bar^{-1}.

Ten simulations were performed of a bilayer consisting of 99 POPC lipids self-assembling around a POPE-cinnamycin complex. The peptide was oriented with its hydrophobic residues pointing in the z direction. POPC lipids were randomly placed around it in a 7 nm x 7 nm x 5 nm box. Afterwards, the box size was increased to 7 nm x 7 nm x 10 nm, 1499 water beads were added, and the system was neutralized with one chloride ion. The setup was simulated for 100 ns with the peptide backbone beads and the NH3 and PO4 bead of the POPE lipid position restrained with a force constant of 1000 kJ/mol/nm^2. This resulted in a bilayer forming around the complex. Two of these simulations were converted to an atomistic representation.

From one of the formed bilayers, a bacterial membrane was generated by randomly mutating lipids to POPE or POPG to give a POPE:POPG ratio of 4:1 in each leaflet. This system was simulated for 3 μs and at each 1 μs the system was converted to an atomistic description resulting in a total of three atomistic descriptions of the cinnamycin-PE complex in a bacterial membrane (*PE_HyAsp_PEPG*).

Hydrogen bond definition

A hydrogen bond was defined to be present when the distance between the donor (D) and the acceptor (A) was less than 3.5 Å and the D-H-A angle was larger than 150º. If all hydrogen of the lipids ammonium group was not observed to form a strong single hydrogen bond, a search for bifurcated (three-centered) hydrogen bonds was performed, which was defined by two hydrogen bond acceptors being within 3.5 Å of the hydrogen bond donor with a D-H-A angle larger than 115º. This angle cutoff was chosen to catch both hydrogen bond acceptors in a bifurcated hydrogen bond.[24] A bifurcated hydrogen bond was often observed between the ammonium group of PE and the HyAsp15 hydroxyl and carboxyl group.

Definition of residue orientations

The orientations of the three investigated groups (HyAsp15 side chain, Phe7(O), and Phe7(NH)) were defined as follows. The side chain of HyAsp/Asp15 (HyAsp in Figure 6 and 7 and Asp in Figure 9) was defined to have its side chain carboxyl group pointing towards the ammonium group of the LysAla19/6 bridge (see Figure 4b) if the χ1 angle was between 0 and 100° (gray in Figure 6, 8 and 9) or else toward the lipid (white). The backbone orientation of Phe7(NH) and Phe7(O) was defined on the basis of the ψ-angle of Ala(N)6 and the ϕ-angle of Gly8, respectively, as these angles were found to describe the dynamic behavior the best. The reason why these angles can describe the orientation of the Phe7(NH) and Phe7(O) orientation lies in the conjugation in the amide system which keeps it in an almost planer configuration resulting in the orientation of e.g. Phe7(NH) being related to the orientation of Ala(N)6(O). Phe7(NH) was thus found to point into the pocket when the ψ-angle of Ala(N)6 was between -130 and 50°, while Phe7(O) was defined to point into the pocket when the ϕ-angle of Gly8 was between 50 and 230° (gray in Figure 6, 8 and 9). Otherwise, it was defined to point out of the pocket (white).

Additional figures

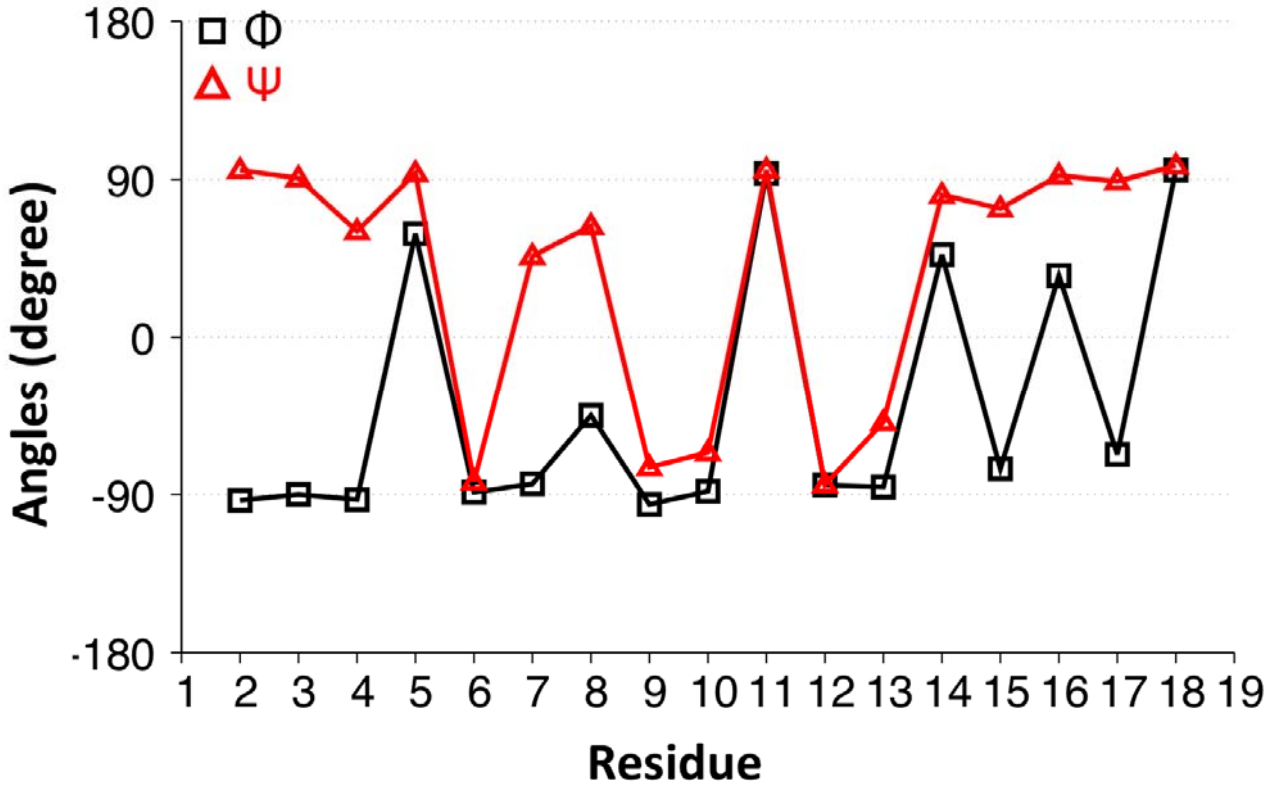

Figure S2. Distribution of phi and psi angles of Cinnamycin in the DMSO environment.

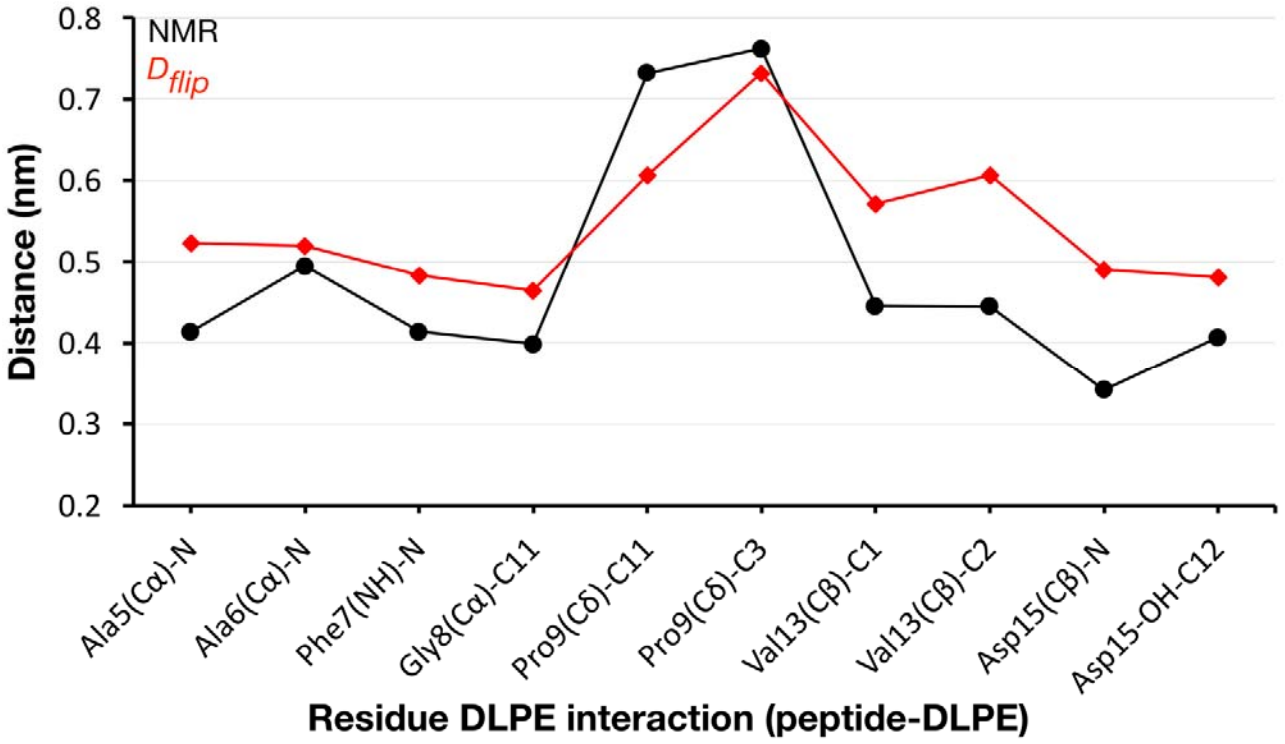

Figure S3. NOE analysis of the Cinnamycin NMR structure[16] (black circles) and the simulated structure (D_{flip}' red rhombus). The residue distance between Cinnamycin and DLPE lipid in the DMSO environment. Lines are guided to the eye.

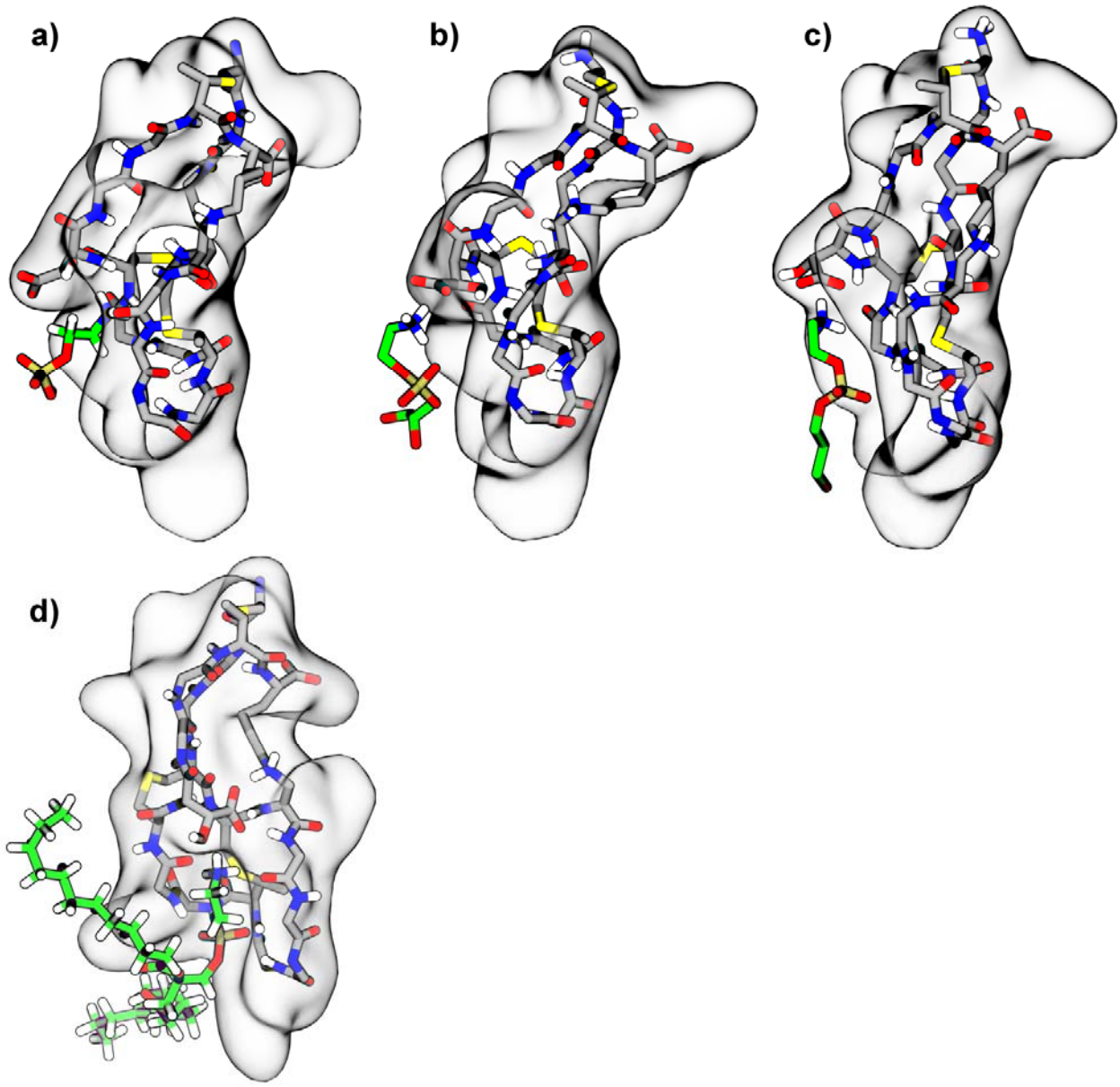

Figure S4. DLPE bound to cinnamycin a) in its initial conformation, b) after minimization, c) after the second equilibration step with NOE restraints applied for a simulation in water showing that a stable complex was not obtained in water, and d) the DLPE bound to cinnamycin after restrained equilibration with the lipid tails shown. Colors and visualization are as described in Figure 5.

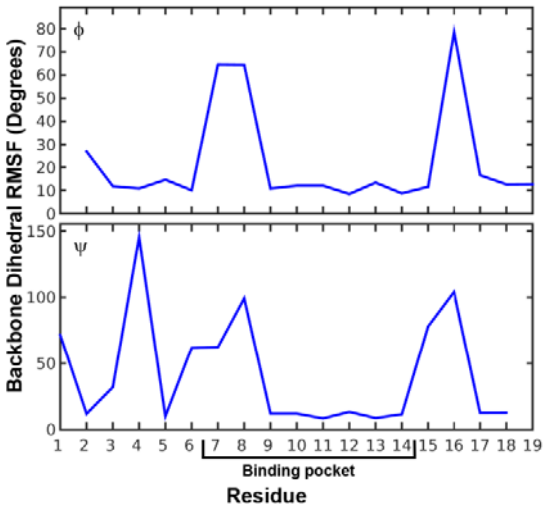

Figure S5. Root mean square fluctuation of cinnamycin with POPE bound (*PE_HyAsp*).

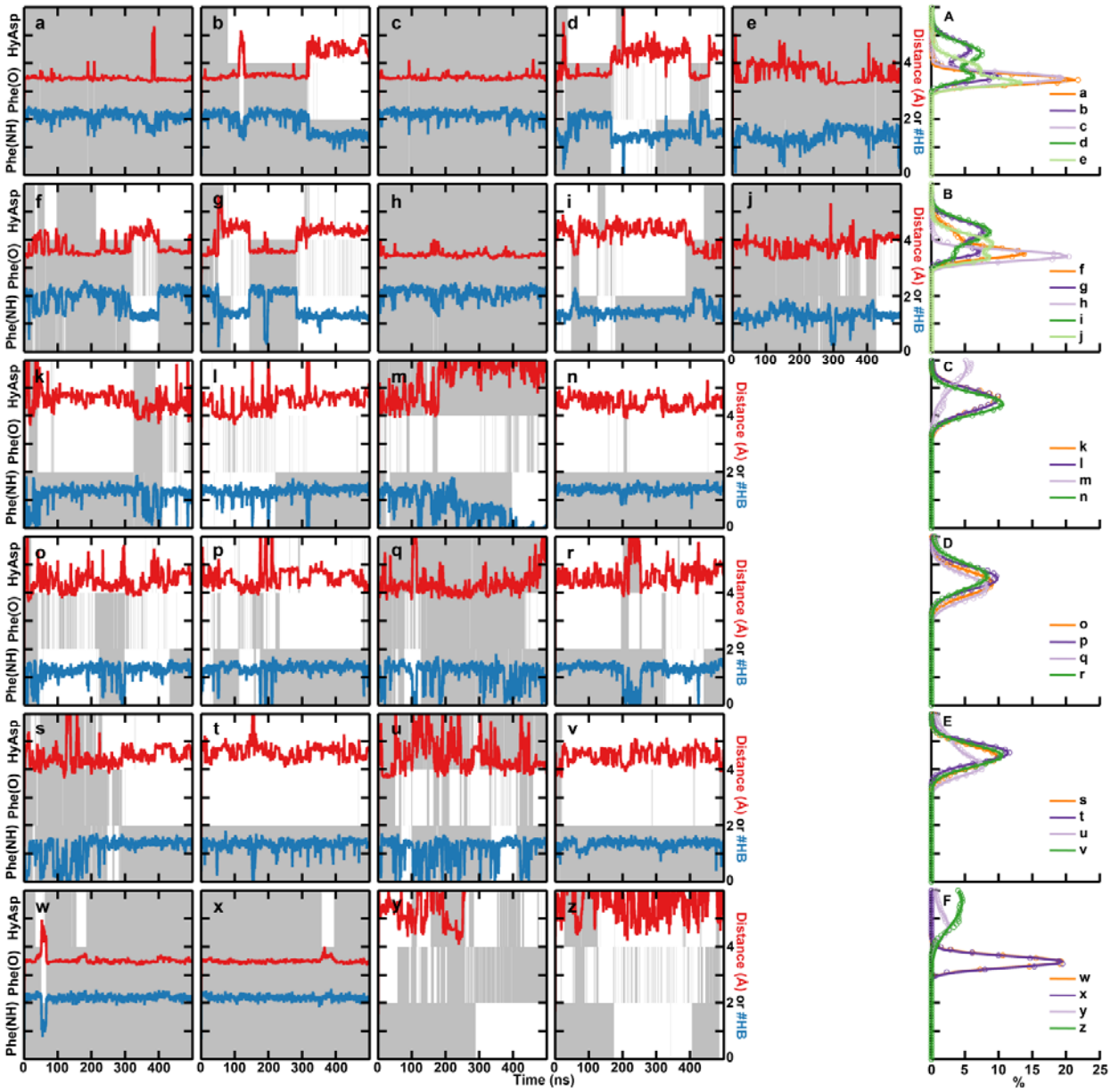

Figure S6. Relation between different interactions and the stability of the binding over time. a-j) POPE, k-v) POmPE, w-x) POPS, y-z) POPC. c,h,m,q,u) the HyAsp side chain was restrained. d,i,n,r,v) cinnamycin HyAsp15Asp mutant. e,j) cinnamycin HyAsp15Asp mutant with side chain restrained. A-F) gives the distribution of the pocket distance over the last 400 ns for the individual simulations.

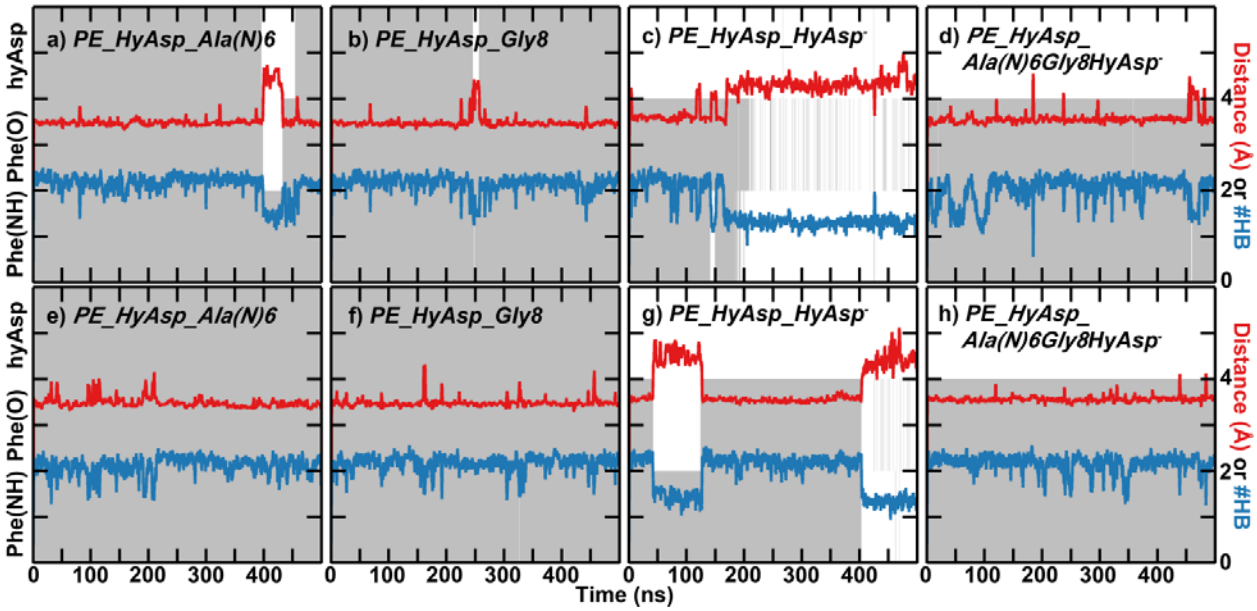

Figure S7. PE-cinnamycin complex with different residues restrained as described by the simulation names (a-h).

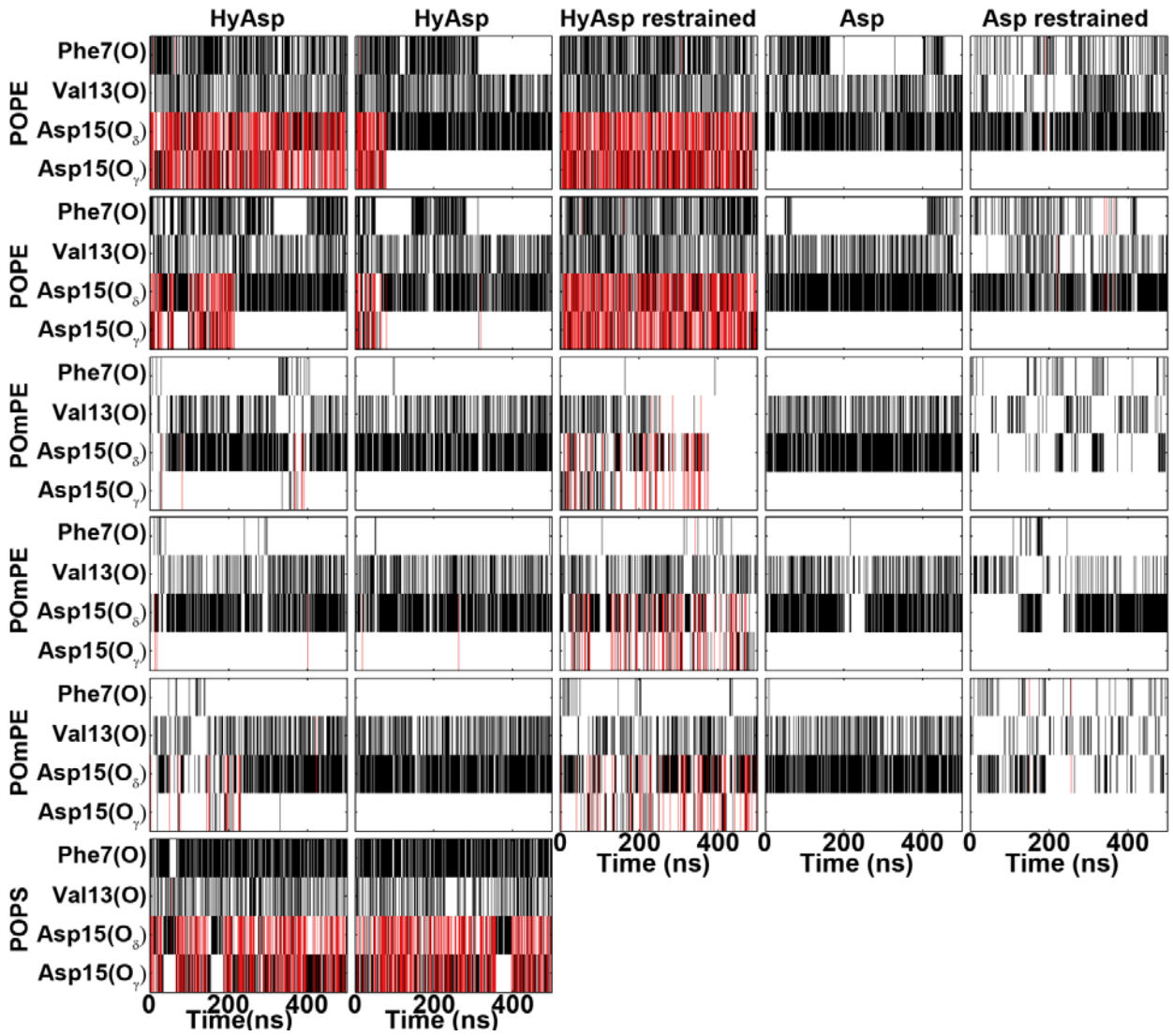

Figure S8. The hydrogen bonds between the lipid amine and the binding pocket. Black lines indicate the presence of standard hydrogen bonds, while red lines indicate the presence of bifurcated hydrogen bonds (two hydrogen bond acceptors for one hydrogen atom). Asp15(O_γ) and Asp15(O_δ) refer to if the hydroxyl and carboxyl oxygens of HyAsp15/Asp15 are involved in a hydrogen bond, respectively.

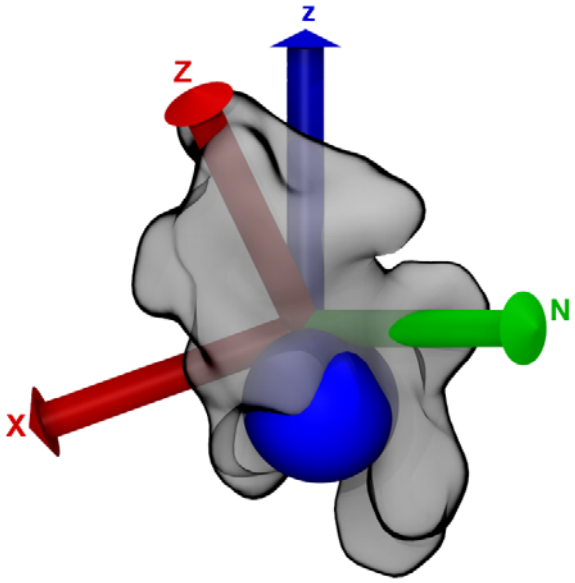

Figure S9. Definition of the orientation of the peptide with respect to the bilayer. The orientation of the peptide in the bilayer was calculated from the Euler angles between the coordinate system of the peptide (X, Y, Z) and the coordinate system of the simulation box (x,y,z). Z was defined as the peptide's principal axis of inertia with the lowest principal moment of inertia, X was defined by the vector perpendicular to Z passing through the sulfur atom of Ala(S)14 and Y was defined as the vector perpendicular to both of them and resulting in formation of a right-handed coordinate system. The line of nodes (N), which is the intersection between the xy and the XY coordinate planes, was defined to be perpendicular to Z and the z-axis of the simulation box (z), in such a way that (z, Z, N) forms a right-handed coordinate system. Because N is always oriented in the bilayers plane the angle between X and N describes the roll angle of the peptide with respect to the bilayer and is thus the angle plotted in Figure 11a. Since the pocket is approximately located at an angle of -90° with respect to X in the XY plane, an angle of 180° is equivalent to the peptide pocket opening pointing directly into the bilayer while an angle of 0° is equivalent to the pocket pointing toward the solvent.

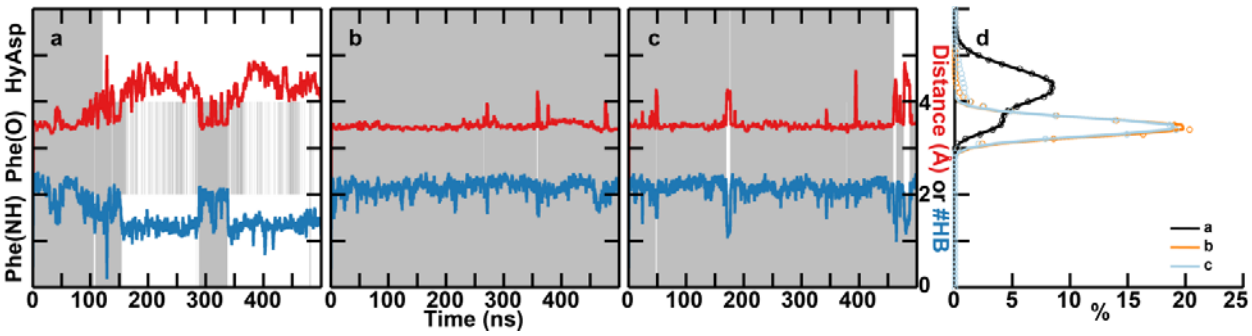

Figure S10. As figure S4 but for the three simulations with POPE bound in bacteria membrane (4:1 POPE:POPG). a-c) plots for the three individual simulations. d) Distance histogram over the last 400 ns of the thee simulations shown in (a), (b), and (c).

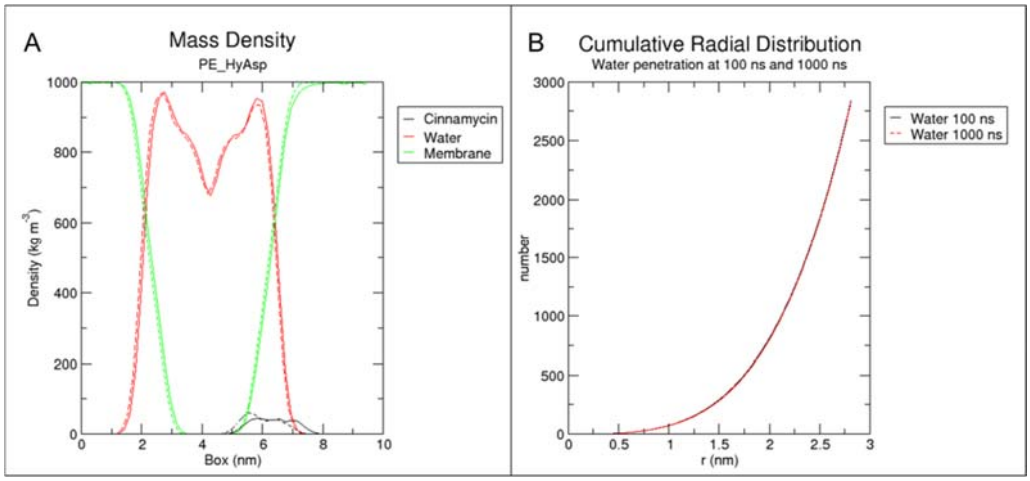

Figure S11. A) Plot comparing early (100-200 ns, full lines) and final (900-1000 ns, dashed lines) mass densities in the system focusing on the protein, membrane and water. We observe little to no changes in membrane thickness or water penetration; though a slight increase in cinnamycin penetration is observed. B) Radial distribution plot showing cumulative water molecules relative to the distance from the center of mass of the membrane. This shows no distinguishable increase in water penetration as a result of cinnamycin exposure.

SI References

(1) Hess, B.; Kutzner, C.; Spoel, D. van der; Lindahl, E. GROMACS 4: Algorithms for Highly Efficient, Load-Balanced, and Scalable Molecular Simulation. *J. Chem. Theory Comput.* 2008, *4*, 435–447.

(2) Pronk, S.; Páll, S.; Schulz, R.; Larsson, P.; Bjelkmar, P.; Apostolov, R.; Shirts, M. R.; Smith, J. C.; Kasson, P. M.; van der Spoel, D.; et al. GROMACS 4.5: A High-Throughput and Highly Parallel Open Source Molecular Simulation Toolkit. *Bioinformatics* 2013, *29* (7), 845–854. https://doi.org/10.1093/bioinformatics/btt055.

(3) Best, R. B.; Zhu, X.; Shim, J.; Lopes, P. E. M.; Mittal, J.; Feig, M.; MacKerell, A. D. Optimization of the Additive CHARMM All-Atom Protein Force Field Targeting Improved Sampling of the Backbone ϕ, ψ and Side-Chain χ_1 and χ_2 Dihedral Angles. *J. Chem. Theory Comput.* 2012, *8* (9), 3257–3273. https://doi.org/10.1021/ct300400x.

(4) Klauda, J. B.; Venable, R. M.; Freites, J. A.; O'Connor, J. W.; Tobias, D. J.; Mondragon-Ramirez, C.; Vorobyov, I.; MacKerell, A. D.; Pastor, R. W. Update of the CHARMM All-Atom Additive Force Field for Lipids: Validation on Six Lipid Types. *J. Phys. Chem. B* 2010, *114* (23), 7830–7843. https://doi.org/10.1021/jp101759q.

(5) Vanommeslaeghe, K.; Hatcher, E.; Acharya, C.; Kundu, S.; Zhong, S.; Shim, J.; Darian, E.; Guvench, O.; Lopes, P.; Vorobyov, I.; et al. CHARMM General Force Field: A Force Field for Drug-like Molecules Compatible with the CHARMM All-Atom Additive Biological Force Fields. *J. Comput. Chem.* 2010, *31* (4), 671–690. https://doi.org/10.1002/jcc.21367.

(6) Vanommeslaeghe, K.; MacKerell, A. D. Automation of the CHARMM General Force Field (CGenFF) I: Bond Perception and Atom Typing. *J. Chem. Inf. Model.* 2012, *52* (12), 3144–3154. https://doi.org/10.1021/ci300363c.

(7) Vanommeslaeghe, K.; Raman, E. P.; MacKerell, A. D. Automation of the CHARMM General Force Field (CGenFF) II: Assignment of Bonded Parameters and Partial Atomic Charges. *J. Chem. Inf. Model.* 2012, *52* (12), 3155–3168. https://doi.org/10.1021/ci3003649.

(8) Durell, S. R.; Brooks, B. R.; Ben-Naim, A. Solvent-Induced Forces between Two Hydrophilic Groups. *J. Phys. Chem.* 1994, *98* (8), 2198–2202. https://doi.org/10.1021/j100059a038.

(9) Neria, E.; Fischer, S.; Karplus, M. Simulation of Activation Free Energies in Molecular Systems. *J. Chem. Phys.* 1996, *105* (5), 1902–1921. https://doi.org/10.1063/1.472061.

(10) Berendsen, H. J. C.; Postma, J. P. M.; van Gunsteren, W. F.; DiNola, A.; Haak, J. R. Molecular Dynamics with Coupling to an External Bath. *J. Chem. Phys.* 1984, *81* (8), 3684–3690. https://doi.org/10.1063/1.448118.

(11) Hoover, W. G. Canonical Dynamics: Equilibrium Phase-Space Distributions. *Phys. Rev. A* 1985, *31*, 1695–1697.

(12) Parrinello, M.; Rahman, A. Polymorphic Transitions in Single Crystals: A New Molecular Dynamics Method. *J. Appl. Phys.* 1981, *52* (12), 7182–7190. https://doi.org/10.1063/1.328693.

(13) Miyamoto, S.; Kollman, P. A. Settle: An Analytical Version of the SHAKE and RATTLE Algorithm for Rigid Water Models. *J. Comput. Chem.* 1992, *13* (8), 952–962. https://doi.org/10.1002/jcc.540130805.

(14) Hess, B.; Bekker, H.; Berendsen, H. J. C.; Fraaije, J. G. E. M. LINCS: A Linear Constraint Solver for Molecular Simulations. *J. Comput. Chem.* 1997, *18* (12), 1463–1472. https://doi.org/10.1002/(SICI)1096-987X(199709)18:12<1463::AID-JCC4>3.0.CO;2-H.

(15) Essmann, U.; Perera, L.; Berkowitz, M. L.; Darden, T.; Lee, H.; Pedersen, L. G. A Smooth Particle Mesh Ewald Method. *J. Chem. Phys.* 1995, *103* (19), 8577–8593. https://doi.org/10.1063/1.470117.

(16) Hosoda, K.; Ohya, M.; Kohno, T.; Maeda, T.; Endo, S.; Wakamatsu, K. Structure Determination of an Immunopotentiator Peptide, Cinnamycin, Complexed with Lysophosphatidylethanolamine by 1H-NMR1. *J. Biochem* 1996, *119*, 226–230.

(17) Wakamatsu, K.; Choung, S. Y.; Kobayashi, T.; Inoue, K.; Higashijima, T.; Miyazawa, T. Complex Formation of Peptide Antibiotic Ro09-0198 with Lysophosphatidylethanolamine:1H NMR Analyses in Dimethyl Sulfoxide Solution. *Biochemistry* 1990, *29* (1), 113–118. https://doi.org/10.1021/bi00453a013.

(18) De Jong, D. H.; Singh, G.; Bennett, W. F. D.; Arnarez, C.; Wassenaar, T. A.; Schäfer, L. V.; Periole, X.; Tieleman, D. P.; Marrink, S. J. Improved Parameters for the Martini Coarse-Grained Protein Force Field. *J. Chem. Theory Comput.* 2013, *9* (1), 687–697. https://doi.org/10.1021/ct300646g.

(19) Marrink, S. J.; Risselada, H. J.; Yefimov, S.; Tieleman, D. P.; Vries, A. H. de; Marrink, S. J.; Risselada, H. J.; Yefimov, S.; Tieleman, D. P.; Vries, A. H. De. The MARTINI Force Field : Coarse Grained Model for Biomolecular Simulations. *J. Phys. Chem. B* 2007, *111* (June), 7812–7824. https://doi.org/10.1021/jp071097f.

(20) Wassenaar, T. A.; Pluhackova, K.; Böckmann, R. A.; Marrink, S. J.; Tieleman, D. P. Going Backward: A Flexible Geometric Approach to Reverse Transformation from Coarse Grained to Atomistic Models. *J. Chem. Theory Comput.* 2014, *10* (2), 676–690. https://doi.org/10.1021/ct400617g.

(21) Morein, S.; Andersson, A.-S.; Rilfors, L.; Lindblom, G. Wild-Type Escherichia Coli Cells Regulate the Membrane Lipid Composition in a Window between Gel and Non-Lamellar Structures. *J. Biol. Chem.* 1996, *271* (12), 6801–6809.

(22) Kabsch, W.; Sander, C. Dictionary of Protein Secondary Structure: Pattern Recognition of Hydrogen-Bonded and Geometrical Features. *Biopolymers* 1983, *22* (12), 2577–2637. https://doi.org/10.1002/bip.360221211.

(23) Bussi, G.; Donadio, D.; Parrinello, M. Canonical Sampling through Velocity Rescaling. *J. Chem. Phys.* 2007, *126* (1), 014101. https://doi.org/10.1063/1.2408420.

(24) Taylor, R.; Kennard, O.; Versichel, W. Geometry of the Nitrogen-Hydrogen...Oxygen-Carbon (N-H...O:C) Hydrogen Bond. 2. Three-Center (Bifurcated) and Four-Center (Trifurcated) Bonds. *J. Am. Chem. Soc.* 1984, *106* (1), 244–248. https://doi.org/10.1021/ja00313a047.